

Measurement of Interfacial Tension from the Shape of a Rotating Drop¹

H. M. PRINCEN, I. Y. Z. ZIA, AND S. G. MASON

Pulp and Paper Research Institute of Canada and Department of Chemistry, McGill University, Montreal 2, Canada

Received March 16, 1966

ABSTRACT

Vonnegut's approximate solution for the shape of a fluid drop in a horizontal rotating tube filled with a liquid of higher density has been extended and numerical solutions based on exact equations have been presented from which it is possible to calculate the interfacial tension from the length of the elongated drop along the axis of rotation when the drop volume, speed of rotation, and density difference between the two phases are known. An experimental method is described and results are given which show good agreement with other methods. The technique is considered to be especially useful for systems in which either phase is highly viscous or viscoelastic. The proposal by Vonnegut that the method be used to measure surface pressure-area curves of insoluble monolayers is shown on theoretical grounds to have limited applicability.

INTRODUCTION

When a fluid drop (phase 1) is placed in a liquid of higher density (phase 2) contained in a rotating horizontal tube it becomes elongated along the axis of rotation until the deformation forces due to the centrifugal field are balanced by the interfacial tension. Vonnegut (1) suggested that this principle be used to measure interfacial tension and developed an approximate theory in which the bubble is considered to be a cylinder with rounded ends. The theory is strictly valid only at high speeds of rotation, but Silberberg (2) improved it by calculating correction factors for low speeds. The method involved measuring the radius of the cylinder and thus required an optical correction factor; this we have found to be a serious limitation. We have extended the theory by using exact equations for the bubble shape and have developed an experimental method based on measuring the bubble length without the need for optical correction

Rosenthal (3) has recently presented similar calculations by a somewhat different method, but his results are less detailed and less suitable for the application considered in this paper.

THEORETICAL PART

It is assumed, as before (1-3), that the angular velocity of rotation ω is sufficiently high that buoyancy due to gravity is negligible and that the drop is aligned on the horizontal axis of rotation. Cylindrical coordinates x, y are chosen (Fig. 1) with origin at the left-hand end of the drop. The angle between the normal of the interface at (x, y) and the negative x -direction is θ , and the semiaxes are x_0 and y_0 ; the densities of the drop and the outer phase are d_1 and d_2 ($d_2 > d_1$) and the interfacial tension is γ . Because of symmetry, it is sufficient to consider only the quarter drop between $0, 0$ and x_0, y_0 . The pressure outside the drop is given by

$$p = p_0 + \frac{d_2 \omega^2 y^2}{2}, \quad [1]$$

¹ This work was supported by the Petroleum Research Fund (PRF 1214-A4).

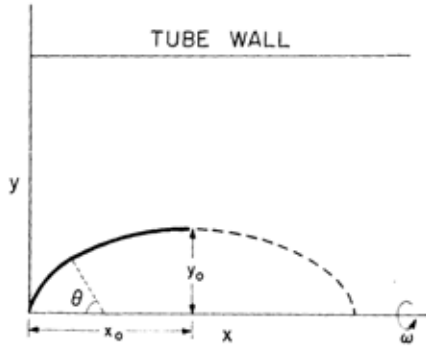


FIG. 1. Coordinate system to describe the shape of a drop rotating about a horizontal axis.

and at $y = 0$ inside the drop by

$$p'_0 = p_0 + \frac{2\gamma}{a}, \quad [2]$$

where a is the radius of curvature of the drop surface at the origin. Thus, at y inside the drop

$$p' = p_0 + \frac{2\gamma}{a} + \frac{d_1 \omega^2 y^2}{2}, \quad [3]$$

so that at the surface

$$\Delta p = p' - p = \frac{2\gamma}{a} - \frac{\Delta d \omega^2 y^2}{2}, \quad [4]$$

where $\Delta d = d_2 - d_1$

The pressure difference is balanced by the capillary pressure across the interface:

$$\Delta p = \gamma \left(\frac{1}{\rho_1} + \frac{1}{\rho_2} \right), \quad [5]$$

where the principal curvatures are

$$\frac{1}{\rho_1} = \frac{d^2 x / dy^2}{[1 + (dx/dy)^2]^{3/2}} = \frac{d \sin \theta}{dy}, \quad [6]$$

and

$$\frac{1}{\rho_2} = \frac{dx/dy}{y[1 + (dx/dy)^2]^{1/2}} = \frac{\sin \theta}{y}. \quad [7]$$

Equating [4] and [5] yields for the equation of interface

$$\frac{d \sin \theta}{dy} + \frac{\sin \theta}{y} = \frac{2}{a} - \frac{\Delta d \omega^2 y^2}{2\gamma}, \quad [8]$$

which can be written in the dimensionless form

$$\frac{d \sin \theta}{dY} + \frac{\sin \theta}{Y} = 2 - \alpha Y^2, \quad [9]$$

where $Y = y/a$, and

$$\alpha = \frac{\Delta d \omega^2 a^3}{2\gamma} = 2ca^3, \quad [10]$$

$$c = \frac{\Delta d \omega^2}{4\nu}. \quad [11]$$

Thus, the shape of the drop is determined by the dimensionless parameter α .

Equation [9] can be integrated to give

$$\sin \theta = Y \left(1 - \frac{\alpha Y^2}{4} \right) \quad [12]$$

or

$$\begin{aligned} \tan \theta &= \frac{dX}{dY} \\ &= \frac{Y \left(1 - \frac{\alpha Y^2}{4} \right)}{\left[1 - Y^2 \left(1 - \frac{\alpha Y^2}{4} \right)^2 \right]^{1/2}}, \end{aligned} \quad [13]$$

where $X = x/a$.

Several useful relations follow readily:

1. When $Y = Y_0$, $\sin \theta = 1$; hence from [12]

$$\alpha Y_0^3 - 4Y_0 + 4 = 0, \quad [14]$$

one of whose roots gives Y_0 as a function of α .

Differentiating [12] yields

$$d \sin \theta = \left(1 - \frac{3\alpha Y^2}{4} \right) dY, \quad [15]$$

which, when multiplied on the left-hand side by $\tan \theta$ and the right-hand side by dX/dY and integrated between the origin and (X_0, Y_0) , yields

$$1 = X_0 - \frac{3\alpha}{4} \int_0^{X_0} Y^2 dX. \quad [16]$$

Since

$$\frac{V}{a^3} = 2\pi \int_0^{X_0} Y^2 dX,$$

where V is the volume of the drop, one finds from [16]

$$\frac{V}{a^3} = \frac{4\pi}{3} \left(\frac{r}{a} \right)^3 = \frac{8\pi}{3\alpha} (X_0 - 1), \quad [17]$$

where r is the radius of a sphere of the same volume as the drop. Equation [17] reduces to a useful form to convert a to r

$$\frac{r}{a} = \left[\frac{2(X_0 - 1)}{\alpha} \right]^{1/3}. \quad [18]$$

3. At high ω the drop is closely approximated by a cylinder with rounded ends. In the cylindrical part $d\sin\theta/dY = 0$, $\theta = 90^\circ$, and $Y = Y_0$ and [9] becomes

$$\alpha Y_0^3 - 2Y_0 + 1 = 0. \quad [19]$$

Combining [19] and [14] yields for a long cylindrical drop

$$Y_0 = 3/2, \quad [20]$$

and the highest possible value

$$\alpha = 16/27. \quad [21]$$

Combining [10], [20] and [21] leads to Vonnegut's equation (1)

$$\gamma = \frac{\Delta d \omega^2 y_0^3}{4}. \quad [22]$$

For the limiting value of α , [13] can be readily integrated to yield for the ends of the cylindrical drop

$$X = \frac{\sqrt{3}}{2} \left[\ln \frac{2\sqrt{9 - Y^2} + 3\sqrt{3}}{2\sqrt{9 - Y^2} - 3\sqrt{3}} - \ln \frac{2 + \sqrt{3}}{2 - \sqrt{3}} \right] + 3 - \sqrt{9 - Y^2}. \quad [23]$$

Since $Y = y/a = 3y/2y_0$, this equation is identical to Vonnegut's equation [16] (1).

For $0 < \alpha < 16/27$, Eq. [13] can be integrated by making the substitution

$$q = 1 - \frac{\alpha Y^2}{4}, \quad [24]$$

to give

$$X = -\frac{1}{\sqrt{\alpha}} \int \frac{q dq}{\left(q^3 - q^2 + \frac{\alpha}{4} \right)^{1/2}} + C. \quad [25]$$

If $q_1 > q_2 > q_3$ are the roots of the cubic term in the denominator it can be shown that

$$q_1 = 1 - \frac{\alpha}{4} Y_0^2. \quad [26]$$

The three roots are always real over the possible range of α , and are conveniently evaluated trigonometrically (4) in the form

$$q_1 = \frac{2}{3} \cos \frac{\psi}{3} + \frac{1}{3},$$

$$q_2 = \frac{2}{3} \cos \left(\frac{\psi}{3} + 240^\circ \right) + \frac{1}{3},$$

$$q_3 = \frac{2}{3} \cos \left(\frac{\psi}{3} + 120^\circ \right) + \frac{1}{3},$$

where

$$\cos \psi = 1 - \frac{27}{8} \alpha.$$

Since the interval of q over which the integral [25] must be evaluated is $q_1 \leq q < 1$, the solution is (5)

$$X = -\frac{2}{\sqrt{\alpha(q_1 - q_3)}} [q_1 F(k, \phi) - (q_1 - q_3) E(k, \phi) + (q_1 - q_3) \tan \phi \sqrt{1 - k^2 \sin^2 \phi}] + C, \quad [27]$$

where F and E are the elliptic integrals of the first and second kind,

$$k^2 = \frac{q_2 - q_3}{q_1 - q_3},$$

and is defined by

$$q = \frac{q_1 - q_2 \sin^2 \phi}{1 - \sin^2 \phi} \left(0 \leq \phi \leq \frac{\pi}{2} \right). \quad [28]$$

At (X_0, Y_0) , q equals q_1 , ϕ equals 0, and the bracketed term in [27] vanishes so that

$$C = X_0. \quad [29]$$

At the origin $X = 0$, $Y = 0$, and $q = 1$

$$X_0 = \frac{2}{\sqrt{\alpha(q_1 - q_3)}} [q_1 F(k, \phi_1) - (q_1 - q_3) E(k, \phi_1) + (q_1 - q_3) \tan \phi_1 \sqrt{1 - k^2 \sin^2 \phi_1}], \quad [30]$$

where $\phi = \phi_1$ when $q = 1$.

These equations allow the drop shape to be computed for any value of α using tables of the elliptic integrals (6). Then all dimensions are known in units of α and can readily be expressed in terms of r using [18].

Instead of α the more convenient shape-determining factor cr^3 can be used by combining [10] and [18]:

$$cr^3 = \frac{\alpha}{2} \left(\frac{r}{a} \right)^3 = X_0 - 1. \quad [31]$$

Table I reports the value of the most important drop parameters for various values of α , and Fig. 2 shows the drop shape for several cases.²

At values of α greater than in Table I (when the central part of the drop is effectively cylindrical) the following equations apply with sufficient accuracy:

$$\alpha = 16/27, \quad [32]$$

and

$$Y_0 = 3/2. \quad [33]$$

From [31]:

$$X_0 = cr^3 + 1. \quad [34]$$

From [31] and [32]:

$$\frac{r}{a} = \frac{2}{3} (cr^3)^{1/3}. \quad [35]$$

From [34] and [35]:

$$\frac{x_0}{r} = \frac{2}{3} \frac{cr^3 + 1}{(cr^3)^{1/3}}. \quad [36]$$

From [33] and [35]:

$$\frac{y_0}{r} = (cr^3)^{-1/3} \text{ or } y_0 = c^{-1/3}. \quad [37]$$

From [36] and [37]:

$$\frac{x_0}{y_0} = \frac{2}{3} (cr^3 + 1). \quad [38]$$

Equation [37] is Vonnegut's (1), but for reasons stated earlier [36] is more useful in experimental work; Fig. 3 shows x_0/r and y_0/r as a function of the independent variable cr^3 .

² For all but the last six values of α in Table I, the shape parameters were calculated by numerical integration of [9], using an IBM 1620 computer. For the highest values of α this procedure was too time-consuming and the table was completed by computing X_0 , Y_0 , r/a , and cr^3 from [30], [26], [18], and [31], respectively.

TABLE I
CALCULATED SHAPE PARAMETERS OF A DROP

α	r/a	Cr^3	x_0/r	y_0/r	x_0/y_0
0	1.000	0	1.000	1.000	1.000
0.05	1.017	0.0263	1.009	0.996	1.013
0.10	1.037	0.0557	1.018	0.990	1.028
0.15	1.058	0.0888	1.029	0.985	1.044
0.20	1.081	0.1265	1.042	0.980	1.063
0.225	1.095	0.1476	1.048	0.976	1.074
0.250	1.108	0.1703	1.056	0.973	1.085
0.275	1.124	0.1951	1.063	0.969	1.098
0.300	1.140	0.2222	1.072	0.965	1.111
0.325	1.158	0.2521	1.082	0.960	1.126
0.350	1.177	0.2854	1.092	0.955	1.143
0.375	1.198	0.3227	1.104	0.950	1.162
0.400	1.222	0.3653	1.117	0.944	1.184
0.425	1.250	0.4146	1.132	0.937	1.209
0.450	1.281	0.4727	1.150	0.928	1.238
0.475	1.318	0.5435	1.171	0.919	1.275
0.500	1.363	0.6330	1.198	0.907	1.321
0.525	1.421	0.7536	1.234	0.892	1.384
0.550	1.504	0.9354	1.287	0.869	1.481
0.555	1.526	0.9854	1.301	0.863	1.508
0.560	1.550	1.043	1.318	0.857	1.539
0.565	1.578	1.111	1.338	0.849	1.576
0.570	1.611	1.192	1.361	0.840	1.621
0.575	1.652	1.296	1.390	0.828	1.678
0.580	1.704	1.435	1.429	0.814	1.756
0.5825	1.737	1.528	1.455	0.804	1.809
0.5850	1.779	1.648	1.488	0.792	1.878
0.5875	1.836	1.817	1.534	0.776	1.977
0.5900	1.925	2.105	1.613	0.751	2.148
0.5910	1.986	2.314	1.669	0.734	2.275
0.5920	2.099	2.739	1.781	0.702	2.538
0.5922	2.150	2.944	1.834	0.688	2.667
0.5924	2.217	3.227	1.907	0.670	2.846
0.5925	2.289	3.555	1.990	0.651	3.059
0.59255	2.355	3.869	2.068	0.634	3.261
0.59257	2.412	4.161	2.140	0.620	3.452
0.59258	2.468	4.453	2.209	0.606	3.645

Silberberg (2) concluded that [37] is applicable when the axis ratio $x_0/y_0 > 3.5$, in general agreement with the present calculations, although the choice of this critical value is arbitrary and depends on the accuracy being sought.

EXPERIMENTAL PART

Apparatus. the rotating cell used (Fig. 4) is driven by a 1/3 hp. a.c. motor (Bodine electric Co. Chicago)

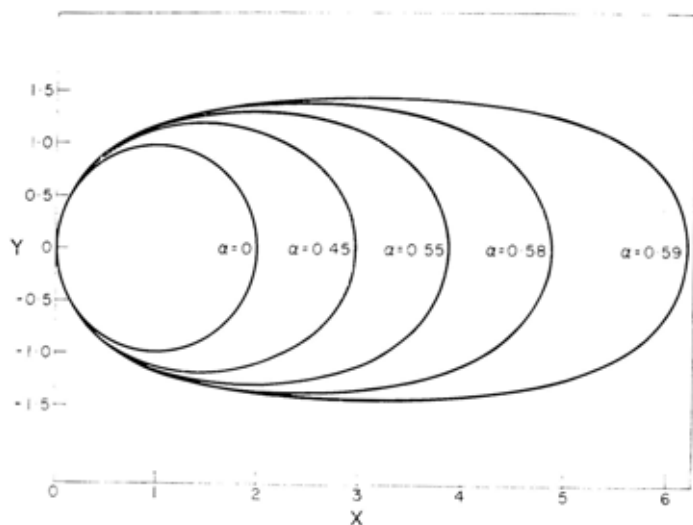


FIG. 2. Shape of a rotating drop for various values of α . The radius of curvature at the drop end serves as the unit of length.

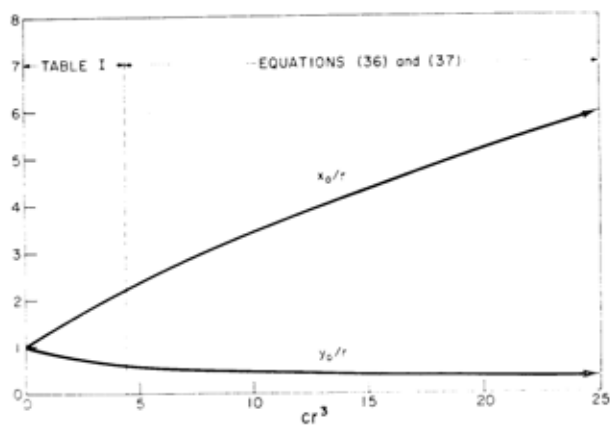


FIG. 3. Variation of x_0/r and y_0/r with cr^3 .

through two DYNA minidrives (Ontario Drive and Gear Ltd.) connected in series so that the speed of rotation of the apparatus is steady and can be varied continuously up to 10,000 r.p.m.; the speed is measured to 1 r.p.m. with a tachometer (Hasler Berne Ltd.).

The glass tube is 1 ± 0.001 cm. i.d. and approximately 22 cm. long. Since it is important to avoid vibration of the bubble, precision bore tubing is used to provide good balancing at all speeds. At each end of the tube there is a ground-glass joint fitted with a stopper. Both stoppers are spring loaded to provide a tight seal. One has a 1.5-mm. capillary in the center (Fig. 4).

Procedure. A critical step in the measurement is the introduction of a bubble of accurately known volume. After thoroughly cleaning the cell, the stopper with the capillary is wetted with the heavier (phase 2) liquid and inserted in one end of the tube. The tube is held vertically and filled completely and allowed to stand so that any trapped air bubbles escape, after which it is inclined nearly horizontally with the open end up. A hypodermic needle fitted to a microburet is slowly inserted through the capillary at the lower end and a carefully measured (to 10^{-4} c.c.) volume of phase 1 is introduced which coalesced to form a single bubble. The needle is slowly withdrawn and the upper open end of the tube is closed with the other stopper, with the excess phase 2 being expelled through the capillary. In this way the drop was introduced under very little hydrostatic pressure. The tube is then inserted in the apparatus clamp.

The bubble length is measured using a horizontal horizontal cathetometer over a range of speeds of rotation.

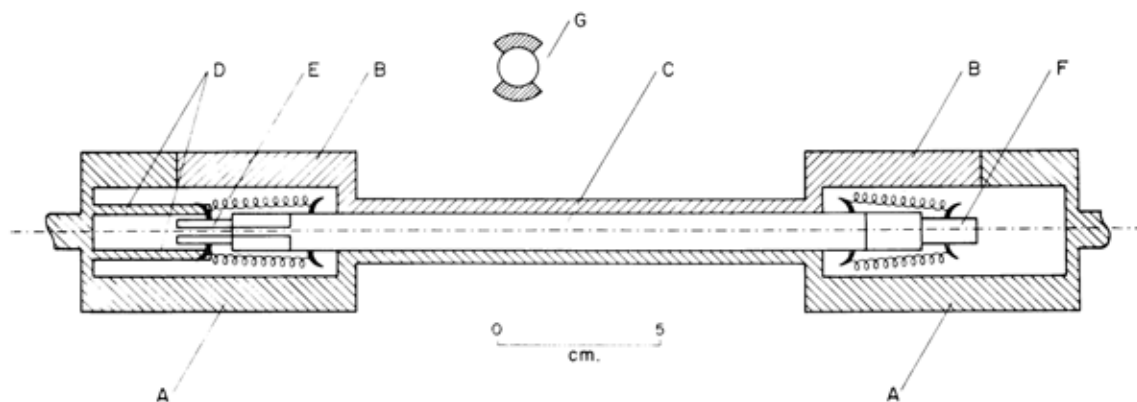


FIG. 4. Rotating drop apparatus (schematic). A—fixed part of clamp assembly, B—removable part of clamp assembly, C—glass tubing, D—two pins to prevent the slip between glass tubing and clamp assembly, E, F—ground-glass stoppers; E has capillary at its center, G—cross section.

After reaching equilibrium the drop length from tip to tip is measured twice at each speed of rotation; from left to right and then in reverse. This reduces any error caused by any inclination of the tube.

RESULTS AND DISCUSSION

In all systems examined, except air and liquids of low viscosity such as water, the drops had very smooth surfaces and as predicted by the theory were elongated along the horizontal axis of rotation with increasing speed of rotation (Fig. 5). A typical set of results and calculations is given in Table II and shows that the method gives constant values of γ over a wide range of ω .

A summary of results for a variety of systems is given in Table III, and some comparisons with the pendant drop and ring tensiometer methods are given in Table IV.

Accurate measurements of ω and V are essential for this method, since γ varies as $\omega^2 V^n$, with $n \geq 3/2$. Of the two requirements the more difficult to meet is the second and it is the reason for the care taken in introducing the bubble into the cell. With a gas bubble, care must be taken to prevent any change of V from variations in temperature and pressure. Although V changes with ω , it is readily shown in bubbles at atmospheric pressure that the variation in V from the centrifugal field is negligible.

It is theoretically possible to determine γ without measuring V , since at high ω [36] is applicable. Substituting [11] into [36] leads to

$$G \left(\frac{1}{\gamma} \right)^{1/3} = H \left(\frac{r^3}{\gamma} \right) + 1, \quad [39]$$

where

$$G = \frac{3x_0}{2} \left(\frac{\Delta t \omega^2}{4} \right)^{1/3}, \quad [40]$$

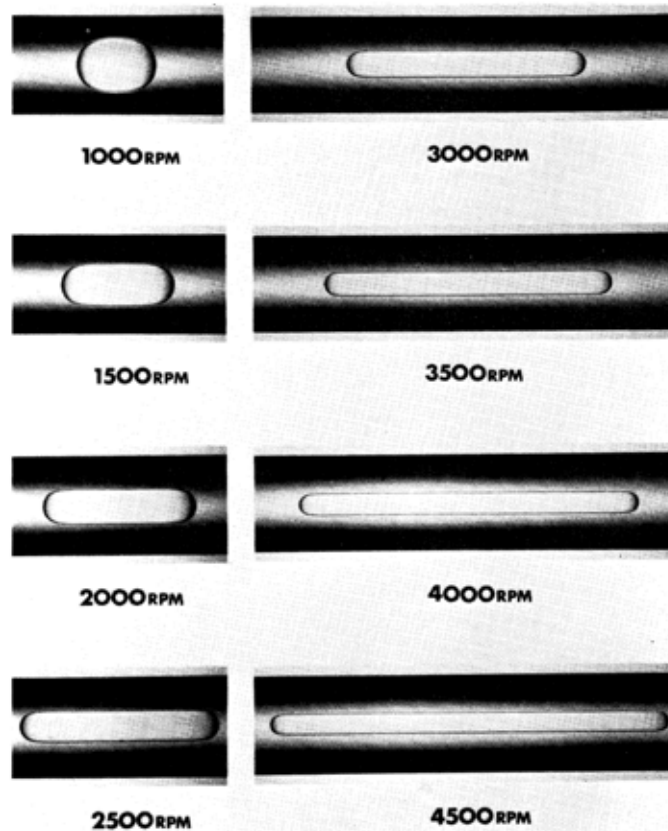


FIG. 5. Photographs of a heptane drop (0.156 cm^3) in glycerol rotating at various speeds.

TABLE II
CALCULATION AND RESULT OF A TYPICAL EXPERIMENT SYSTEM: n-HEXADECANE / GLYCEROL

$$V = 0.1900 \text{ cm.}^3 \quad \Delta d = 0.485 \text{ g. cm.}^{-3} \quad r = 0.3567 \text{ cm.}$$

(r.p.m.)	ω	$2 x_0(\text{cm.})$	x_0/r	Cr^3 ^a	$c (\text{cm.}^{-3})$	γ ^b (dyne cm^{-1})
	(rad, sec^{-1})					
859	89.9	1.048	1.469	1.580	34.84	28.14
1207	126.4	1.343	1.883	3.163	69.74	27.77
1629	170.6	1.786	2.504	5.72	126.1	27.97
1957	204.9	2.172	3.045	8.22	181.3	28.08
2160	226.2	2.433	3.411	10.05	221.6	27.99
2454	256.9	2.819	3.952	12.90	284.4	28.13
2644	276.8	3.091	4.334	15.05	331.9	27.99
2947	308.6	3.530	4.949	18.70	412.3	28.00
3285	343.9	4.062	5.695	23.47	517.5	27.71
3639	381.0	4.579	6.420	28.36	625.3	28.14
4020	420.9	5.200	7.290	34.65	764.0	28.12
4489	470.0	5.996	8.406	43.27	954.1	28.06

Mean = 28.0

S.D. = 0.6%

^a Interpolated values from x_0/r using Table I when $x_0/r < 2.209$. For greater values [36] is used.

^b Calculated from [11].

TABLE III
INTERFACIAL TENSION AND OTHER PHYSICAL PROPERTIES OF EXPERIMENTAL SYSTEMS

No.	Phase 1	Phase 2	$\Delta d (\text{g cm.}^{-3})$	$\eta_2(\text{poises})$	γ^b (dyne cm^{-1})
1	Air	Glycerol	1.260	8	66.1
2	Heptane	Glycerol	0.576	8	28.4
3	n-Hexadecane	Glycerol	0.485	8	28.0
4	Water	Cyclohexanol phthalate	0.071	230	26.4
5	Water	Dow Corning fluorosilicone fluid FS-1265	0.302	130	40.3
6	Air	2% aqueous solution of Cyana-mer P250 polyacrylamide	1.001		65.3

TABLE IV
COMPARISON OF INTERFACIAL TENSION MEASUREMENT BY DIFFERENT METHODS
(Temperature: $21^\circ \pm 1^\circ\text{C}$)

System	γ^b (dyne cm.^{-1})		T	γ_1/γ_2
	Rotating drop (1)	Pendant drop (2)		
Air/glycerol	66.1	64.6	63.4	1.02
Heptane/glycerol	28.4	27.8	27.7	1.02
n-Hexadecane/glycerol	28.0	27.2	27.3	1.03

and

$$H = \frac{\Delta d \omega^2}{4}. \quad [41]$$

If the drop length is measured at two or more speeds, both the V and γ can be calculated from simultaneous equations such as

$$\left. \begin{aligned} G_1 \left(\frac{1}{\gamma} \right)^{1/3} &= H_1 \left(\frac{r^3}{\gamma} \right) + 1 \\ G_2 \left(\frac{1}{\gamma} \right)^{1/3} &= H_2 \left(\frac{r^3}{\gamma} \right) + 1 \end{aligned} \right\} \quad [42]$$

It can easily be shown that the solutions of [42] are

$$\gamma = \left[G_1 - H_1 \left(\frac{G_1 - G_2}{H_1 - H_2} \right) \right]^3, \quad [43]$$

and

$$\begin{aligned} r^3 &= \left(\frac{G_1 - G_2}{H_1 - H_2} \right) \\ &\cdot \left[G_1 - H_1 \left(\frac{G_1 - G_2}{H_1 - H_2} \right) \right]^2 \\ &= \left(\frac{G_1 - G_2}{H_1 - H_2} \right) \gamma^{2/3}. \end{aligned} \quad [44]$$

However, this method was found to be impractical, because the ratio $G_1(H_1 - H_2) / H_1(G_1 - G_2)$ was never much greater than unity. Thus, a small error in ω , and hence in G and H , leads to a large error in γ .

In accord with Vonnegut's observation (1) an air bubble in water had a rippled surface. Although the exact cause of the ripples is not known, it occurred only with systems of low viscosity and was probably due to the vibration from the motor drive.

Rayleigh (7) showed that in a nonrotating field a cylindrical drop develops axisymmetric standing waves of length exceeding the circumference with an accompanying decrease in interfacial area. More closely related to present work is the investigation by Rosenthal (3), who found that a long bubble subjected to small axisymmetric disturbances in the axial direction is stable at all wavelengths if the ratio $[(y_0)_a / (y_0)_b] \geq 0.63$, where $(y_0)_a$ is the actual radius of the cylinder and $(y_0)_b$ is the equilibrium value given by [37]. It then follows readily from [37] that if there is a sudden change from ω_1 to ω_2 the bubble will not break up provided that $\omega_2 / \omega_1 \geq 0.50$. In our experiments no instability was observed when ω was changed gradually or kept constant. A sudden stop of the apparatus, however, often resulted in the breakup of the cylinder into two or more smaller drops in accordance with Rayleigh's theory (7, 8).

It should be remembered that ω is the speed of rotation of the drop. Because of buoyancy, the drop axis does not coincide exactly with the axis of rotation so that ω of the drop may be slightly less than that of the tube.

Thus, by assuming $\omega_{\text{drop}} = \omega_{\text{tube}}$ an error may be introduced to yield a higher value of γ ; this may explain why the values obtained were consistently higher than those by the ring and pendant drop methods (Table IV). One would expect, however, that this error would disappear at high ω and / or η_2 .

It should be pointed out that viscosity does not enter into the theory, although in a very viscous system it takes longer for the drop to reach its equilibrium shape. Thus this method is particularly useful for viscous systems where, by contrast, the more conventional techniques may not be applicable.

Two non-Newtonian aqueous systems, one pseudoplastic and the other viscoelastic, were briefly examined. After 3 hours rotation at 2025 r.p.m. an air bubble in a 0.1 % solution of Carbopol 940 (Goodrich Chemical) reached a steady but not an equilibrium x_0 which depended upon whether the final speed was reached by increasing or decreasing ω ; this is presumably due to the high yield value of the pseudoplastic Carbopol solution. However, an air bubble in a viscoelastic polyacrylamide solution (2 % Cyanamer P250, American Cyanamid) after 3 hours rotation at 1530 r.p.m. reached an equilibrium x_0 from which γ was evaluated (Table III). Thus, this method may be applicable to viscoelastic molten polymer systems.

CONCLUDING REMARKS

Vonnegut (1) suggested that the method might be used to measure surface pressure-area curves of insoluble monolayers, since the surface area A of the drop given by

$$\frac{A}{a^2} = 4\pi \int_0^{Y_0} Y \sqrt{1 + (dX/dY)^2} dy, \quad [45]$$

can be controlled by changing W . Substituting for dX/dY from [13] yields,

$$\frac{A}{a^2} = 4\pi \int_0^{Y_0} \frac{Y dY}{\left[1 - Y^2 \left(1 - \frac{\alpha Y^2}{4} \right)^2 \right]^{1/2}} \quad [46]$$

and making the substitution

$$q = 1 - \frac{\alpha Y^2}{4},$$

one obtains

$$\frac{A}{a^2} = -\frac{4\pi}{\sqrt{\alpha}} \int_1^{q_1} \frac{dq}{\left(q^3 - q^2 + \frac{\alpha}{4}\right)^{1/2}}, \quad [47]$$

which integrates to (5)

$$\frac{A}{a^2} = \frac{8\pi}{\sqrt{\alpha(q_1 - q_3)}} F(k, \phi_1), \quad [48]$$

where the symbols have the same meaning as in [30].

When $cr^3 = 0$, the drop is spherical and $A/r^2 = 4\pi = 12.57$. For much higher values of cr^3 the area of the cylindrical drop is given approximately by

$$\frac{A}{r^2} = \frac{8\pi}{3} \frac{cr^3 + 1}{(cr^3)^{2/3}}. \quad [49]$$

Thus, at $cr^3 = 29$, axis ratio x_0/y_0 is 20, but the surface area has only doubled. The variation in surface area produced by changing the speed of rotation is therefore too small to be used in evaluating a surface pressure-area isotherm.

LIST OF SYMBOLS

a	= radius of curvature of the drop surface at the origin.
A	= surface area of the drop.
c	= a parameter defined by [11].
d_1, d_2	= density of phase 1 (drop) and phase 2.
Δd	= $d_2 - d_1$.
E, F	= elliptic integral of the second and first kinds.
G, H	= defined by [40] and [41].
k	= modulus of elliptic integral.
p, p_0	= pressure outside the drop; at $y = 0$.
p', p'_0	= pressure inside the drop; at $y = 0$.
q_1, q_2, q_3	= roots of cubic equation (see [47]).
r	= radius of a sphere of the same

volume as the drop.

x, x_0	= cylindrical coordinate; semi major axis.
X	= x/a .
y, y_0	= cylindrical coordinate; semi minor axis.
Y	= y/a .
V	= volume of drop.
α	= parameter defined by [10].
γ	= interfacial tension.
η	= viscosity.
θ	= the angle between the normal of the interface at (x, y) and the negative x -direction.
ρ_1, ρ_2	= principal radii of curvature of drop surface.
ϕ	= amplitude of elliptic integral.
ω	= angular velocity.

REFERENCES

- VONNEGUT, B., *Rev. Sci. Instr.* **13**, 6 (1942).
- SILBERBERG, A., Ph.D. Thesis, Basel University, Switzerland, 1952.
- ROSENTHAL, D. K., *J. Fluid Mech.* **12**, 358 (1962).
- "Handbook of Chemistry and Physics," 40th ed., p. 259. Chemical Rubber Publishing Co., Cleveland, 1958.
- GROBNER, W., AND HOFREITER, N., "Integral-tafel," 3rd ed., Vol. I, p. 78. Springer Verlag, Vienna, 1961.
- EMDE, F., "A. M. Legendres Tafeln der Elliptischen Normalintegrale." Konrad Wittwer, Stuttgart, 1931.
- RAYLEIGH, LORD, *Proc. London Math. Soc.* **10**, 4 (1879).
- RUMSCHEIDT, F. D., AND MASON, S. G., *J. Colloid Sci.* **17**, 260 (1962).